

II.G.9 USD Catalysis Group for Alternative Energy*

James D. Hoefelmeyer (Primary Contact),
Ranjit Koodali, Grigoriy Sereda, Dan Engebretson,
Jan Puszynski, Jacek Swiatkiewicz, Hao Fong,
Phil Ahrenkiel, Rajesh Shende

The University of South Dakota (USD)
414 E. Clark St.
Vermillion, SD 57069
Phone: (605) 677-6186
E-mail: jhoefelm@usd.edu

DOE Managers

HQ: Eric Miller
Phone: (202) 287-5829
E-mail: Eric.Miller@hq.doe.gov

GO: David Peterson
Phone: (720) 356-1747
E-mail: David.Peterson@go.doe.gov

Contract Number: DE-EE0000270

Subcontractor:

South Dakota School of Mines and Technology,
Rapid City, SD

Project Start Date: December 1, 2009
Project End Date: November 30, 2011

*Congressionally directed project

Fiscal Year (FY) 2011 Objectives

- Synthesize dye-sensitized TiO₂ nanorods with catalyst particles attached to the tips.
- Use Langmuir-Blodgett methods to incorporate nanorods as membrane-spanning units in lipid bilayers.
- Develop and test a prototype capillary reactor for photocatalysis of water-splitting.
- Synthesize high-surface area carbon nanofelt.
- Develop and test a prototype hydrogen fuel cell with carbon nanofelt incorporated as catalyst support material.

Technical Barriers

This project addresses the following technical barriers from the Photoelectrochemical Hydrogen Production and Fuel Cells sections of the Fuel Cell Technologies Program Multi-Year Research, Development and Demonstration Plan:

3.1.4 Photoelectrochemical Hydrogen Production

- (Y) Materials Efficiency
- (Z) Materials Durability

- (AA) PEC Device and System Auxiliary Material
- (AB) Bulk Materials Synthesis
- (AC) Device Configuration Designs
- (AD) Systems Design and Evaluation

3.4 Fuel Cells

- (A) Durability
- (B) Cost
- (C) Performance

Technical Targets

TABLE 1. Technical Targets: Photoelectrochemical Hydrogen Production (from Table 3.1.10)

Characteristics	Units	2006 status	2013 target
Usable semiconductor bandgap	eV	2.8	2.3
Chemical conversion process efficiency	%	4	10
Plant solar-to-hydrogen efficiency	%	Not available	8
Plant durability	hr	Not available	1,000

Our strategy is to utilize TiO₂ as semiconductor (bandgap ~3.0 eV) that is dye-sensitized with visible light chromophore such as N719 dye (~1.7 eV). Ideally, the chromophore would be a broad-spectrum absorber to allow utilization of near infra-red (NIR) and visible light. Our project does not focus specifically on dye improvement, only utilization of established sensitization protocols. Dye-sensitization has the advantage that band-edge potentials can match requirements for component half-reactions of water-splitting while utilizing the solar spectrum (visible/NIR photons).

TABLE 2. Technical Targets: H₂ Fuel Cell (Transportation)

Characteristics	Units	2010 target	2015 target
Durability with cycling ^{a,b}	Hr	5,000	5,000
Cost ^a	\$/kW _e	45	30
Cost ^b	\$/kW _e	25	15

^a Integrated transportation fuel cell power systems operating on direct hydrogen.

^b Transportation fuel stacks operating on direct hydrogen.

FY 2011 Accomplishments

- Synthesis of anisotropic TiO₂ anatase nanocrystal with growth in <100>, <101>, or <001> direction with organo-carboxylate or organo-amine surface agent.

- Synthesis of mesoporous silica doped with Ti or W ions and demonstration of photocatalytic proton reduction in aqueous solution with methanol. Hydrogen turnover frequency was $0.0002 \text{ H}_2 \cdot \text{tungsten site}^{-1} \cdot \text{s}^{-1}$ ($220 < \lambda < 380 \text{ nm}$ transmitted).
- Synthesis of TiO_2 nanotube array double-layer. Pt nanoparticles were deposited on the TiO_2 surface. Demonstration of photocatalytic proton reduction in aqueous solution with methanol or iodide. Hydrogen evolution was $0.37 \text{ mL} \cdot \text{s}^{-1} \cdot \text{m}^{-2}$ ($220 < \lambda < 400 \text{ nm}$ transmitted).
- Electrospinning of polymer nanofibers, ceramic nanofibers, and thermal treatment to yield graphitic carbon nanofibers.
- Acquisition of Langmuir-Blodgett trough, total organic carbon analyzer, graphitization furnace, gas chromatograph, and fuel cell test station as part of South Dakota research infrastructure improvement effort.



Introduction

There is demand for abundant energy without consequences of pollution that can be met with solar energy utilization. While there are many ways to use sunlight, we focus on the use of materials that allow fast conversion of light to hydrogen and fast conversion of hydrogen to electricity. These two processes can be accomplished with two types of devices, a photoelectrochemical cell and hydrogen fuel cell, respectively. Both processes are complex, and research into their optimization is a priority. Our research into photoelectrochemical cells is an effort to develop new materials that can produce hydrogen from sunlight and water at high efficiency and low cost; our research into hydrogen fuel cells will mostly focus on development of new materials to make a longer-lasting and lower cost device.

Approach

Photoelectrochemical cells include catalysts that rapidly capture sunlight and convert the energy to a chemical fuel and chemical oxidizer. This can be done by ‘splitting’ water to hydrogen and oxygen. More specifically, water undergoes autodissociation to give protons and hydroxide anions. If electrons are added to protons, then hydrogen is synthesized; while taking away electrons from hydroxide anions yields oxygen. The catalyst speeds up these two chemical processes. The catalyst must also be able to absorb sunlight. Upon doing so, the light energy causes the excitation of an electron. The electron is more reactive after excitation, and it leaves an electron ‘hole’. The catalyst must be able to use the excited electron to synthesize hydrogen and to use the electron hole to synthesize oxygen. So far, no single material has been discovered that can accomplish all three tasks: light absorption, hydrogen synthesis, and oxygen

synthesis. Combination of several materials, however, working together can enable the photoelectrochemical cell. This is somewhat similar to photosynthesis, wherein plants convert sunlight to fuel (sugars) and oxidizer (oxygen), in that several molecular pieces work together. For this reason, photocatalysis within a photoelectrochemical cell is sometimes referred to as artificial photosynthesis. The materials that we plan to use include nanocrystals of TiO_2 , Pt, and RuO_2 , dye molecules, and lipids. The materials will be organized in chemical reactions and self-assembly steps to produce a reactive free-standing membrane capable of solar photocatalysis in which water is converted to hydrogen and oxygen.

Hydrogen fuel cells catalyze the reverse reaction of photoelectrochemical cells that split water. Instead of giving back a photon; however, the fuel cell produces electricity. Thus hydrogen (fuel) and oxygen (oxidizer) combine in a membrane-electrode assembly to produce water and electric current. The membrane-electrode assembly includes cathode, anode, and proton exchange membrane. At the anode, hydrogen gives up electrons to form protons. At the cathode, electrons and protons that formed at the anode combine with oxygen to form water. The protons reach the cathode through the proton exchange membrane. The electrons reach the cathode through an external circuit. The reaction at the cathode is the driving force for the fuel cell, and force the flow of electrons through the external circuit thereby producing electric current. The hydrogen fuel cell has many material components, and these are susceptible to degradation that limits the utility, lifetime, and value of the fuel cell. Our work is focused making new materials for the electrodes that extend the lifetime. We plan to use carbon nanofelts composed of carbon nanofibers. The carbon nanofibers can be produced upon thermal graphitization of polymer or ceramic (metal carbide) electrospun nanofibers.

Results

TiO_2 nanorods were synthesized via solvothermal synthesis. The nanorods were characterized with electron microscopy, powder X-ray diffraction (XRD), ultraviolet (UV)-visible and luminescence spectroscopy (Figure 1). Powder X-ray diffraction data indicated presence of anatase crystallites with broadened peaks. The 004 reflection had less line broadening than other reflections in the powder pattern, which is evidence of the anisotropic nature of the crystal. The electron microscopy data show the presence of high aspect ratio nanorods. High resolution micrographs show presence of lattice fringes that indicate the highly crystalline nature of the nanorod. The TiO_2 nanorods disperse in non-polar solvents such as hexane. The dispersion, in hexane, was used for spectroscopic analysis. The nanorods absorb strongly in the UV spectrum, with the unusual feature that the absorbance is blue-shifted by 100 nm compared to bulk anatase. This effect is due to quantum confinement in the crystal in which the Bohr exciton radius is less than the diameter of the nanorod

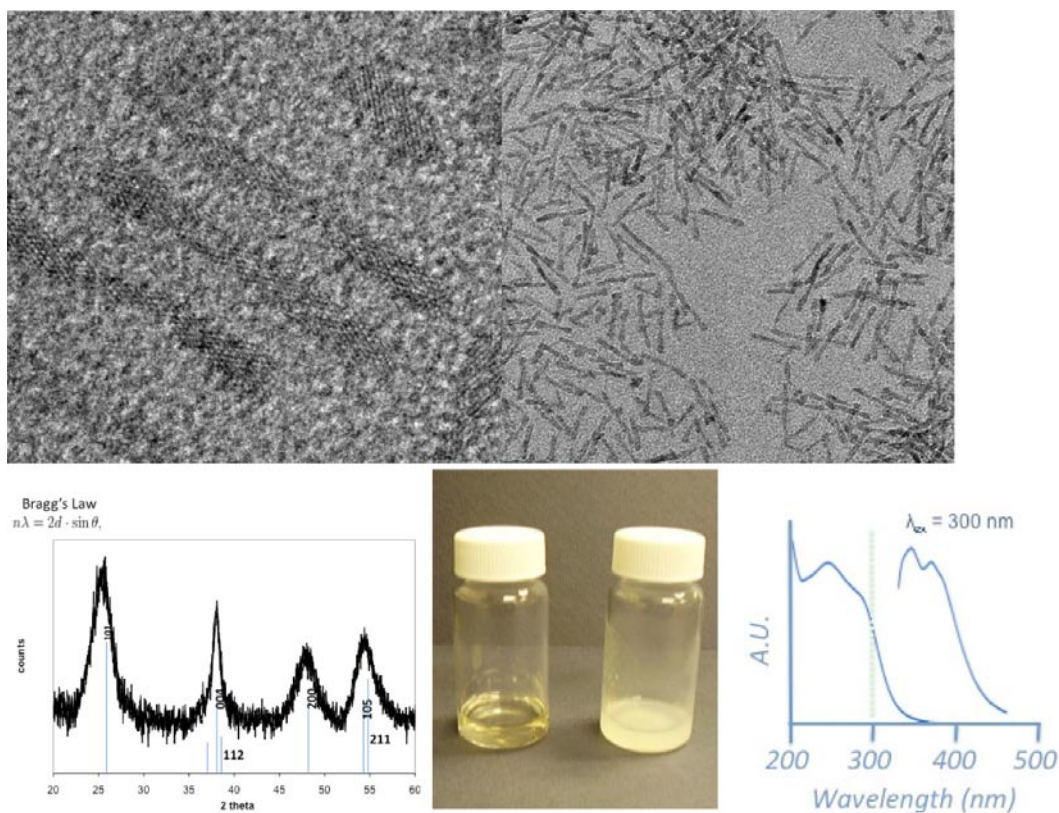


FIGURE 1. Characterization data of TiO_2 nanorods: (top) transmission electron micrographs, (bottom, from left to right) powder XRD, NR dispersion before and after exposure to visible light for 24 hrs, UV-visible and luminescence spectra.

(the effect was independent of nanorod length in the four fractions). The emission spectrum was recorded upon excitation at 300 nm. The TiO_2 nanorod dispersion is light sensitive. Over the course of several hours under visible light exposure, a white precipitate formed; whereas, dispersions protected from visible light exposure were stable for months. More recently, the growth of the anisotropic nanocrystal could be controlled to limit growth in $\langle 100 \rangle$, $\langle 101 \rangle$, or $\langle 001 \rangle$ directions dependent on conditions during synthesis.

We have attempted surface modification of the TiO_2 nanorods (NRs). One approach is selective nucleation of metal nanoparticles on the NR tips. The NRs were dispersed in high boiling solvent into which a metal precursor ($\text{Pt}(\text{acac})_2$ or $\text{Co}_2(\text{CO})_8$) was injected. The reactions led to formation of metal nanocrystals in solution; however, the nucleation did not occur on the NR tips (Figure 2). Another approach has been ligand exchange on the nanorods. TiO_2 NR were exposed to a solid support with dopamine chains. The NRs were attached to the surface of the support concomitant to displacement of linoleic acid. This may be due to two factors: 1) the chelating nature of the catecholate group may bind the TiO_2 surface more tightly, and 2) entropically, the reaction is favored due to the preorganization of ligands on the solid support. The solid support was washed to remove unbound TiO_2

NRs. The dopamine terminus of the solid support can be readily cleaved with trifluoroacetic acid, thereby liberating dopamine stabilized TiO_2 NRs. This was confirmed with transmission electron microscopy and nuclear magnetic resonance.

Synthesis of ordered mesoporous TiO_2 thin-film was performed using evaporation induced self assembly (EISA) and supercritical CO_2 assisted infusion methods. In EISA, a dilute solution containing Ti-butoxide, Pluronic123, HCl (38% in water), and butanol was spin coated on a glass substrate. The coated substrates were aged for 24 hr in a controlled humidity environment at 25°C. Films after aging were calcined at 350°C for 2 hr to remove the surfactant. In supercritical CO_2 infusion method, a glass substrate pre-coated with the Pluronic F108 surfactant film was loaded inside a PARR reactor, and it was heated to 60°C and pressurized to 3,000 psi with CO_2 . At these processing conditions, a known amount of Ti-butoxide followed by water was injected into the reactor. As a result, solubilized portion of Ti-precursor in supercritical CO_2 was infused and hydrolyzed inside the solid surfactant film coated on a substrate. After 1 hr, the reactor was depressurized and cooled down to room temperature and the substrates were removed and calcined at 350°C. The films synthesized by both methods were characterized by scanning electron microscopy (SEM), atomic force microscopy (AFM), X-ray

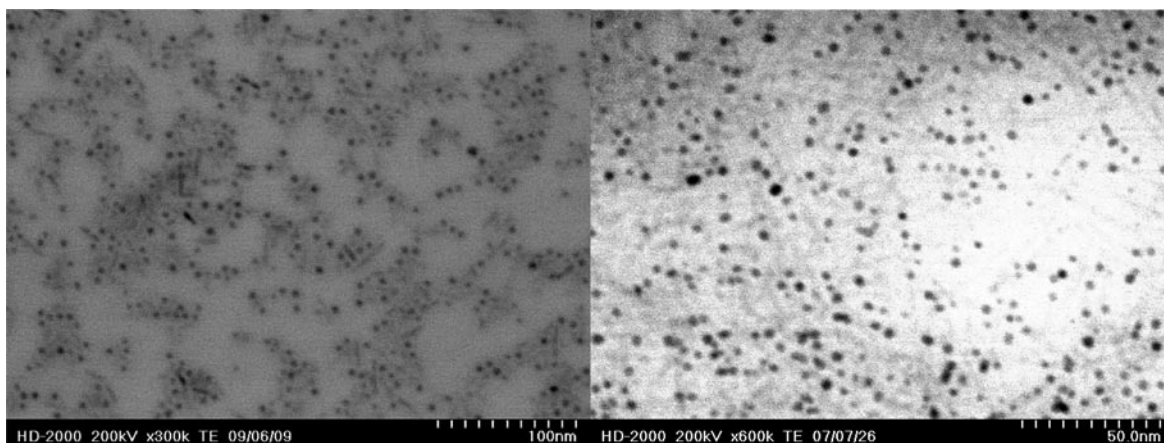


FIGURE 2. Nucleation of metals in the presence of TiO_2 NRs so far led to mixtures of metal nanocrystals and TiO_2 NRs with no evidence of metal-semiconductor interface: (left) Co nanoparticles and TiO_2 NRs (right) Pt nanoparticles and TiO_2 NRs.

diffraction, surface area, and ellipsometry. SEM images of TiO_2 film prepared by EISA reveal ordered mesoporous structure with three-dimensional cubic and two-dimensional hexagonal pore ordering with the d-spacing of 18.50 nm and 18 nm, respectively as determined by fast Fourier transform analysis. AFM images indicate highly ordered structure of the mesopores and partial pore ordering in the TiO_2 thin-films synthesized using supercritical CO_2 -assisted infusion. The smaller size pores as evident in SEM and AFM images may provide mass transfer limitation for charge transport. Consequently, experiments were performed to increase pore size using pore swelling agent; for instance, 1,3,5 trimethyl benzene. Crack-free ordered mesoporous TiO_2 thin films with different thickness were prepared using EISA method. The film thickness ranges from 400 nm to 3,100 nm depending on number of layers coated and the average refractive index for these films was 1.5 as determined by ellipsometry.

We successfully demonstrated that Ti-MCM-48 mesoporous materials can be used for the photosplitting of water to generate hydrogen. Furthermore, the coordination state of Ti in the MCM-48 materials could be easily controlled by changing the order of addition of the Ti precursor. Ti-MCM-48 catalysts were tested for photocatalytic hydrogen. We extended this preparative method for the synthesis and characterization of WO_3 dispersed on MCM-48 materials and found that the photocatalytic evolution of hydrogen is dependent on the loading of WO_3 . The long-range ordered mesoporous structure of MCM-48 was well preserved after tungsten incorporation. Tungsten oxide species were highly dispersed in MCM-48 matrix and no bulk crystalline WO_3 was formed. The as-prepared W-MCM-48 materials show notable photocatalytic activity for hydrogen evolution from methanol-water mixture under UV irradiation though commercial bulk WO_3 is not active for the reaction. The photocatalytic mechanism was studied by electron spin resonance spectroscopy. The tungsten oxide species that are

highly dispersed in MCM-48 matrix possess a suitable band gap and sufficient reduction potential for the photocatalytic reduction of H_2O to generate H_2 .

Efforts were made on the fabrication of double-sided TiO_2 nanotube membrane using electrochemical anodization method. Double sided TiO_2 nanotubes were grown using Ti foil (25 μm thick, 99.7% purity) purchased from Alfa Aesar. Ti sheet was degreased by sonicating sequentially in acetone, ethanol, and de-ionized water, followed by drying in a nitrogen stream. Electrochemical anodization of titanium was carried out at ambient conditions using a two-electrode system and a direct current power supply (Agilent Technologies, 0-60 V). Degree of anodization of Ti metal was controlled by limiting anodization voltage and H_2O content in the electrolyte. For anodization an organic electrolyte containing 0.3 wt% NH_4F and 2 vol% water in ethylene glycol was used. A platinum gauge electrode was used as a cathode in all the experiments. After anodization, the sample was washed in water to remove the impurities. The double sided TiO_2 nanotubes membrane was sensitized with 0.1 M dilute aqueous salt solution of hexachloroplatanic acid and sonicated for 5 minutes and finally annealed in argon environment containing 10 vol% H_2 at 400°C for 1 hr. The SEM image of annealed Pt/ TiO_2 nanotubes is shown in Figure 3A whereas SEM image for the cross section of double sided TiO_2 nanotube membrane is depicted in Figure 3B. These images revealed tube length of about 17 μm on both side of etched Ti metal foil.

Hydrogen generation by photocatalysis using double-sided TiO_2 nanotubes membrane sensitized with Pt was investigated. This membrane was placed in a quartz cell containing aqueous solution with methanol or iodide, degassed with Ar, and irradiated with a 500 W high pressure Xe lamp equipped with AM 1.5G and IR filter (220 nm < λ < 400 nm). Gas samples from the head space of the quartz cell were withdrawn periodically using a gas syringe and analyzed using a gas chromatograph equipped

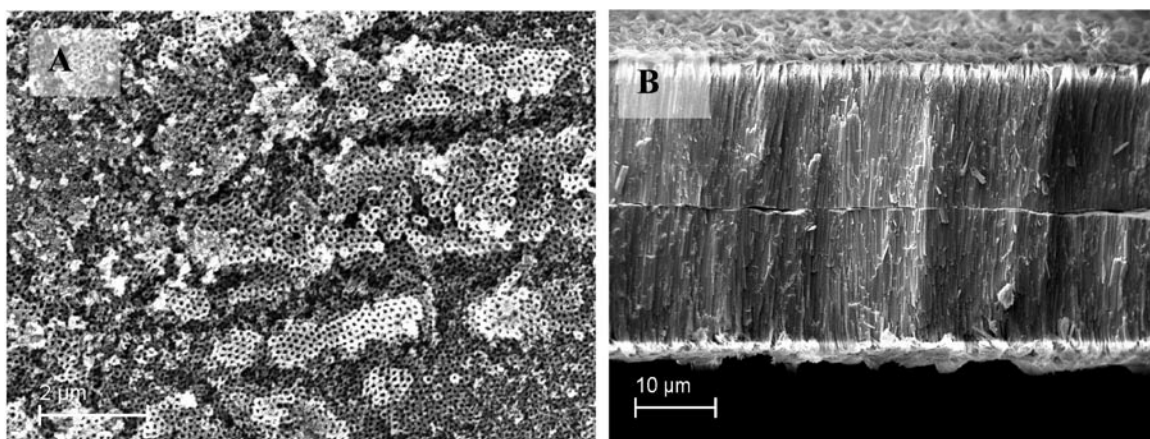


FIGURE 3. SEM images of A) TiO_2 nanotubes sensitized with Pt and B) cross section of double-sided TiO_2 nanotube membrane.

with a thermal conductivity detector. Hydrogen evolution rate was $0.37 \text{ mL} \cdot \text{s}^{-1} \cdot \text{m}^{-2}$.

Nonwoven fabrics made of electrospun polyacrylonitrile (PAN) polyvinyl alcohol, and titania carbide (TiC)-based carbon nanofibers, dubbed as Electrospun Carbon Nanofelt, with extremely high specific surface areas (up to $2,200 \text{ m}^2/\text{g}$) and other desired morphological and structural properties (e.g. high graphitic crystallinity), were synthesized. Conditions during electrospinning affect morphology of the polymer fibers such as diameter and porosity. Thermal treatment leads to carbon nanofibers (graphitization occurs at higher temperatures with retention of morphology). For example, electrospun PAN was graphitized thermally to yield carbon nanofibers (Figure 4). Owing to the unique morphology and structures, the electrospun carbon nanofelt is expected to out-perform carbon black as the catalyst support.

Conclusions and Future Directions

The work on photocatalyst materials for solar hydrogen involves use of high surface area TiO_2 to which functional

materials on the surface enable photocatalytic water splitting. So far, several forms of high surface area TiO_2 were obtained: ordered mesoporous thin film, nanorod, nanotube arrays, or single site Ti (or W) on SiO_2 -MCM-41. While doped MCM-41 was shown to catalyze proton reduction in aqueous solution, the materials still require catalyst sites and visible-light chromophore. Platinized TiO_2 nanotube arrays did show H_2 evolution under UV irradiation. So far, attempts toward selective nucleation of metals (Co or Pt) on the tips of TiO_2 NRs have proven unsuccessful despite reports in the literature. Thus one key challenge is the controlled organization of functional surface features on the TiO_2 . Future work will include:

- Ligand exchange on the surface of TiO_2 nanostructures.
- Selective nucleation of metal (Co, Pt, Ru) on TiO_2 NR tips with new surface ligands.
- Sensitization of TiO_2 nanostructures with visible light chromophores.
- Photocatalyst evaluation (under simulated solar radiation) with attention to quantify turnover frequency.

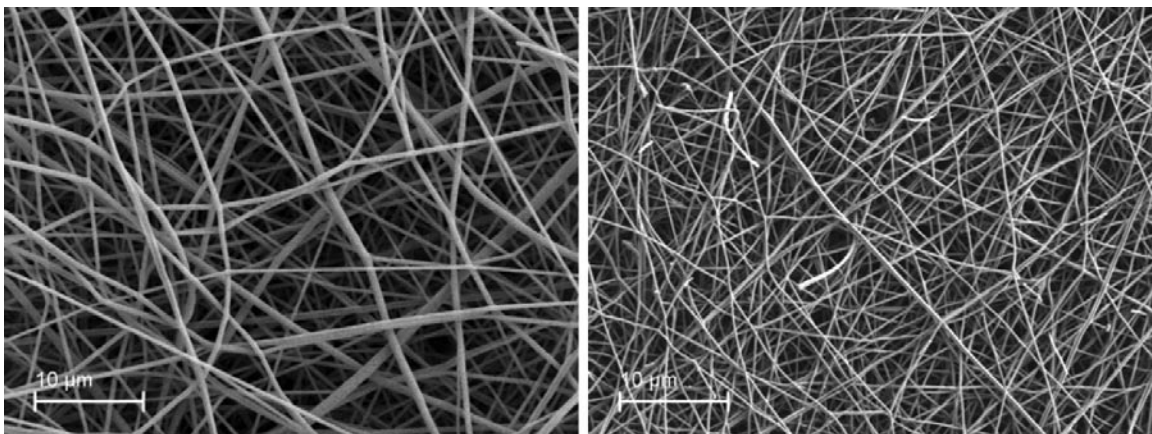


FIGURE 4. PAN-based electrospun nanofibers (left) and PAN-based carbon nanofibers (right).

The work toward carbon nanofelt for catalyst support in hydrogen fuel cell has been quite fruitful. Electrospinning of polymers is a viable technique to large-scale synthesis of nanofibers with tunable morphological properties. The polymer fibers could be graphitized to make carbon nanofibers with retention of morphology. Also, electrospun ceramic nanofibers could be produced, including TiC. Chemical oxidation of TiC led to extraction of the metal and formation of graphitic carbon nanofibers. The carbon nanofibers could show improved performance in working fuel cell environment. Future work will include:

- Construct a fuel cell that utilizes carbon nanofelt as electrode material (catalyst support).
- Test the prototype fuel cell.

Patents Issued

1. Qiquan Qiao, Hao Fong, Prakash Joshi, Lifeng Zhang, and David Galipeau. "TiO₂ Nanofiber/Nanoparticle Mixture Anode for Highly Efficient Dye Sensitized Solar Cells", patent in application.

FY 2011 Publications/Presentations

1. S. Budhi, H.S. Kibombo, D. Zhao, A. Gonshorowski, R.T. Koodali 'Synthesis of titania-silica xerogels by co-solvent induced gelation at ambient temperature' *Mater. Lett.* 2011 (published online Apr. 22, 2011) DOI: 10.1016/j.matlet.2011.04.054.
2. V. Presser, L. Zhang, J.J. Niu, J. McDonough, C. Perez, H. Fong, Y. Gogotsi 'Flexible Nano-felts of Carbide-Derived Carbon with Ultra-high Power Handling Capability' *Adv. Ener. Mater.* 2011 (published online Apr. 15, 2011) DOI: 10.1002/aenm.201100047.
3. S. Banerjee, A. Horn, H. Khatri, G. Sereda 'A green one-pot multicomponent synthesis of 4H-pyrans and polysubstituted aniline derivatives of biological, pharmacological, and optical applications using silica nanoparticles as reusable catalyst' *Tetra. Lett.* 2011, 52(16), 1878-1881.
4. H.S. Kibombo, D. Zhao, A. Gonshorowski, S. Budhi, M.D. Koppang, R.T. Koodali 'Cosolvent-Induced Gelation and the Hydrothermal Enhancement of the Crystallinity of Titania-Silica Mixed Oxides for the Photocatalytic Remediation of Organic Pollutants' *J. Phys. Chem. C* 2011, 115(13), 6126-6135. DOI: 10.1021/jp110988j.
5. C. Lai, G. Zhong, Z. Yue, G. Chen, L. Zhang, A. Vakili, Y. Wang, L. Zhu, J. Liu, H. Fong 'Investigation of post-spinning stretching process on morphological, structural, and mechanical properties of electrospun polyacrylonitrile copolymer nanofibers' *Polymer* 2011, 52(2), 519-528. DOI: 10.1016/j.polymer.2010.11.044.
6. S. Banerjee, V. Balasanthiran, R.T. Koodali, G. Sereda 'Pd-MCM-48: a novel recyclable heterogeneous catalyst for chemo- and regioselective hydrogenation of olefins and coupling reactions' *Org. Biomol. Chem.* 2010, 8, 4316-4321. DOI: 10.1039/C0OB00183J.
7. G. Sereda, V. Rajpara 'Photoactivated and photopassivated benzylic oxidation catalyzed by pristine and oxidized carbons' *Catal. Comm.* 2011, 12(7), 669-672. DOI: 10.1016/j.catcom.2010.12.027.
8. G. Sereda, V. Rajpara 'Exploration of Solid-Supported Reactions with Gold Nanoparticles' *J. Chem. Ed.* 2010, 87(9), 978-980.
9. D. Zhao, A. Rodriguez, N.M. Dimitrijevic, T. Rajh, R.T. Koodali 'Synthesis, Structural Characterization, and Photocatalytic Performance of Mesoporous W-MCM-48' *J. Phys. Chem. C* 2010, 114, 15278-15734.
10. L. Zhang, J. Hu, A.A. Voevodin, H. Fong 'Synthesis of Continuous TiC Nanofibers and/or Nanoribbons Through Electrospinning Followed by Carbothermal Reduction' *Nanoscale* 2010, 2, 1670-1673.
11. Z.C. Wu, Y. Zhang, T.X. Tao, L. Zhang, H. Fong 'Silver nanoparticles on amidoxime fibers for photo-catalytic degradation of organic dyes in waste water' *Appl. Surf. Sci.* 2010, 257, 1092-1097.
12. J. Liu, Y. Tian, Y. Chen, J. Liang, L. Zhang, H. Fong 'A surface treatment technique of electrochemical oxidation to simultaneously improve the interfacial bonding strength and the tensile strength of PAN-based carbon fibers' *Mater. Chem. Phys.* 2010, 122(2-3), 548-555.
13. D. Zhao, S. Budhi, A. Rodriguez, R.T. Koodali 'Rapid and facile synthesis of Ti-MCM-48 mesoporous material and the photocatalytic performance for hydrogen evolution' *Int. J. Hydrogen Ener.* 2010, 35(11), 5276-5283.
14. S. Wen, L. Liu, L. Zhang, Q. Chen, L. Zhang, H. Fong 'Hierarchical electrospun SiO₂ nanofibers containing SiO₂ nanoparticles with controllable surface-roughness and/or porosity' *Mater. Lett.* 2010, 64(13), 1517-1520.
15. Z. Zhou, K. Liu, C. Lai, L. Zhang, J. Li, H. Hou, D.H. Reneker, H. Fong 'Graphitic carbon nanofibers developed from bundles of aligned electrospun polyacrylonitrile nanofibers containing phosphoric acid' *Polymer*, 2010, 51(11), 2360-2367.
16. J.H. Son, M.A. Pudenz, J.D. Hoefelmeyer 'Reactivity of the Bifunctional Amphiphilic Molecule 8-(dimesitylboryl)quinoline: Hydrolysis and Coordination to CuI, AgI and PdII' *Dalton Trans.* 2010, DOI: 10.1039/C0DT00798F.
17. R.T. Koodali, D. Zhao 'Photocatalytic degradation of aqueous organic pollutants using titania supported periodic mesoporous silica' *Energy Environ. Sci.* 2010, 3, 608-614.
18. V. Rajpara, S. Banerjee, G. Sereda 'Iron Oxide Nanoparticles Grown on Carboxy-Functionalized Graphite: An Efficient Reusable Catalyst for Alkylation of Arenes' *Synthesis*, 2010, 16, 2835-2840. DOI: 10.1055/s-0029-1218851
19. P. Joshi, L. Zhang, D. Davoux, L. Liu, D. Galipeau, H. Fong, Q. Qiao 'Nanofiber/Nanoparticle Composites for Highly Efficient Dye Sensitized Solar Cells', *Energy Environ. Sci.* 2010, 3, 1507-1510.